2nd URSI AT-RASC, Gran Canaria, 28 May – 1 June 2018

Determining all ambiguities in direction of arrival measured by radar systems

Daniel Kastinen
Swedish Institute of Space Physics (IRF), Box 812, SE-98128 Kiruna, Sweden
Umeå University, Department of Physics, SE-90187 Umeå, Sweden

Abstract

When using radar systems to determine the position and motion of objects, there is an ambiguity problem. This ambiguity manifests itself for certain sensor configurations when determining the Direction Of Arrival (DOA) of an incoming electromagnetic plane wave onto the radar. Depending on the sensor positions in space, a radar system can respond the same way for several different plane wave DOAs, thereby making it impossible to determine the true DOA. Therefore we have developed a mathematical framework and a practical method to find all ambiguities in any multichannel radar. We have used a set intersection viewpoint to formulate an alternative form for the solutions to the ambiguity problem. The new formulation allows for an efficient implementation using the numerical Moore-Penrose inverse to find all ambiguities and approximate ambiguities. This definition led to the discovery of noise-induced ambiguities in theoretically ambiguity-free radars. Finally, we explore the possibility to use the sensor gain patterns to resolve ambiguities and restrict the elevation angle of a detection. This study originated in the need to resolve ambiguous meteor trajectories in data from the Middle and Upper Atmosphere Radar in Shigaraki, Japan. We have therefore used this radar as a practical example throughout the paper. Our results and methods can be used to classify ambiguities in any radar system, to design new radar systems, to improve trajectory estimation using statistical information and to identify possibly faulty DOA calculations and correct them.

1 Introduction

Ever since Heinrich Hertz in 1886 showed that radio waves could be reflected from solid objects, the concept of radars have profoundly impacted science. The reflected radar signal, or echo, is an electromagnetic plane wave and its Direction Of Arrival (DOA) can be used to detect and discern position and motion. There are a plethora of methods available today to determine the DOA onto a multichannel radar. However, the "ambiguity problem" sheds doubt on DOA measurements [1, 4]. This doubt boils down to a single problem: that a signal output from a radar system could have been caused by several different DOAs. Determining DOAs is critical in many research fields today. For example in radar meteor science, DOA measurements are used to calculate precise meteoroid trajectories and orbits [3]. This study originated in the need to resolve ambiguous meteor head echo DOAs in data from the Middle and Upper Atmosphere Radar (MU-radar) in Shigaraki, Japan, but the same techniques are also used to track satellites and space debris. Being able to trust these DOA measurements is of vital importance if the data is to be used in simulations and consequent research, such as Monte Carlo-type simulations of meteor showers and their parent bodies [2].

Therefore we have developed a mathematical framework and a practical method to find all ambiguities and approximate ambiguities in any multichannel radar system. We have also examined ambiguities induced by noise in theoretically ambiguity-free radars. Finally, we explored the possibility of using the sensor gain patterns to resolve ambiguities.

2 Mathematical framework

We define the mathematical equivalent of a radar system by considering N antenna groups consisting of n_j antennas each. These antennas have positions in space, denoted as $\mathbf{h}_{jk}$, where the group is indexed by j and the antenna indexed by k. By combining the n_j signals from these antennas in each group, the radar system will output N signals, forming N sensors. We define the sensor positions as the geometric center $\mathbf{r}_j$ of the antenna groups, $\mathbf{r}_j = \frac{1}{n_j}\sum_{k=1}^{n_j}\mathbf{h}_{jk}$.

These N sensors will describe a measurement of an electromagnetic plane wave as a set of complex numbers $\mathbf{x} \in \mathbb{C}^N$. By simulating how these sensors respond to a wave in a sensor response model, one can extract information about the incoming wave. The sensor response model as a function of DOA is

$$\mathbf{x}(\mathbf{k}) = \begin{pmatrix} Ae^{-i\langle \mathbf{k},\mathbf{r}_1\rangle_{\mathbb{R}^3}} \\ \vdots \\ Ae^{-i\langle \mathbf{k},\mathbf{r}_N\rangle_{\mathbb{R}^3}} \end{pmatrix} = \sum_{j=1}^{N} \hat{\mathbf{e}}_j A e^{-i\langle \mathbf{k},\mathbf{r}_j\rangle_{\mathbb{R}^3}}. \quad (1)$$

Ambiguities arise when a sensor response model responds

the exact same way for different incoming waves, thus making it impossible to tell the events apart. If the sensor response model has the property that: for all the wave DOAs it never maps distinct DOAs to the same sensor response, then it is an injective function. Applying the definition of an injective function onto our sensor response model yields

$$R(\mathbf{k}_2 - \mathbf{k}_1) = 2\pi\mathbf{I}. \tag{2}$$

Where $\mathbf{I} \in \mathbb{Z}^N$ is an integer vector and $R \in \mathbb{M}^{N\times 3}$ a matrix. The matrix R is defined with the sensor positions $\mathbf{r}_j$ as row vectors $\mathbf{r}_j^T$ where ^{T} denotes the transpose. This derivation was first performed to find the uniqueness and linear independence of steering vectors in array space [1], although not from the injective function viewpoint, but for the same reasons of describing ambiguity. These equation were never explicitly solved, instead conditions for ambiguity-free configurations were derived based on inequalities. These conditions have been used to design new radar systems but they exclude many ambiguity-free radars. The conditions are also not useful for classifying ambiguities in radar systems as they are a binary indication of the existence of ambiguity.

3 Solution

3.1 Theoretical ambiguity set

The solution to equation 2 is divided into two steps. The first step is to find the solution for all wave vector differences, $\mathbf{s} = \mathbf{k}(\theta_1,\phi_1) - \mathbf{k}(\theta_2,\phi_2)$. Inserting $\mathbf{s}$ into equation 2 gives

$$R\mathbf{s} = 2\pi\mathbf{I}. \tag{3}$$

Theorem 1: The solution set Ω of $\mathbf{s}$'s to equation 3 can be found as a set of surface intersections $\Omega = \bigcap_{j=1}^{N} \left(\bigcup_{k=f_j^{\min}}^{f_j^{\max}} \mathbb{P}_{jk} \right)$ where $f_j^{\max} = \left\lfloor 2\frac{|\mathbf{r}_j|}{\lambda} \right\rfloor$ and $f_j^{\min} = -\left\lceil 2\frac{|\mathbf{r}_j|}{\lambda} \right\rceil$. The surfaces that we union are circular plane sections, or disks, defined as $\mathbb{P}_{jk} = \{\mathbf{x} \in \mathbb{R}^3 : |\mathbf{x}| \leq \frac{4\pi}{\lambda}, \langle \mathbf{x} + \mathbf{p}_{jk}, \mathbf{n}_j \rangle = 0\}$ where the plane normal is defined as $\mathbf{n}_j = \frac{\mathbf{r}_j}{|\mathbf{r}_j|}$ and the displacement point is defined as $\mathbf{p}_{jk} = \frac{k\lambda}{|\mathbf{r}_j|}\mathbf{n}_j$.

3.2 Numerical ambiguity set

The advantage of using the viewpoint of plane intersections to find the integer solutions is that it can reduce the numerical algorithm to one that is often efficient. We first manipulate the result from *Theorem 1* by using the property that set intersection is distributive over set union, i.e. $A \cap (S \cup T) = (A \cap S) \cup (A \cap T)$ for all sets A, S, T. Thus the set Ω can be rewritten as $\Omega = \bigcap_{j=1}^{N} \left(\bigcup_{k=f_j^{\min}}^{f_j^{\max}} \mathbb{P}_{jk} \right) = \bigcup_{k_1=f_1^{\min}}^{f_1^{\max}} \cdots \bigcup_{k_N=f_N^{\min}}^{f_N^{\max}} \bigcap_{j=1}^{N} \mathbb{P}_{jk_j}$. Calculating all the terms $\bigcap_{j=1}^{N} \mathbb{P}_{jk_j}$ is impractical since it would require an N plane intersection calculation for $\prod_{j=1}^{N}(f_j^{\max} - f_j^{\min})$ permutations. However, for any set A, $\emptyset \cap A = \emptyset$. Thus if any pair within $\mathbb{P}_{1k_1} \cap \cdots \cap \mathbb{P}_{Nk_N}$ is the empty set, that entire term will be the empty set. And we know that for any set A, $\emptyset \cup A = A$. Thus every term containing two planes not intersecting can be disregarded.

We will take advantage of the above described property to exclude unnecessary calculations. To perform this exclusion, first define a N_J plane intersection as $\mathscr{I}_J = \bigcap_{j=1}^{N_J} \mathbb{P}_{jk_j}$ where J is an indexing set. J is defined as $J = \{f_j^{\min} \leq k_j \leq f_j^{\max} : 1 \leq j \leq N_J,\ j \in \mathbb{Z}, k_j \in \mathbb{Z}\}$, i.e. a set of N_J integer solutions for the first 1 through N_J sensors. $\mathscr{I}_J$ can thus describe all terms and partial terms, where a full term is described by $N_J = N$. The intersection $\mathscr{I}_J$ can be calculated with linear algebra by $\mathscr{I}_J = \{\mathbf{s} \in \mathbb{R}^3 : W_J\mathbf{s} = \mathbf{b}_J\}$, where $W_J = \begin{pmatrix} \mathbf{n}_1^T \\ \mathbf{n}_2^T \\ \vdots \\ \mathbf{n}_{N_J}^T \end{pmatrix}, \mathbf{b}_J = \begin{pmatrix} -\langle \mathbf{n}_1, \mathbf{p}_{1k_1} \rangle \\ \vdots \\ -\langle \mathbf{n}_{N_J}, \mathbf{p}_{N_J k_{N_J}} \rangle \end{pmatrix}$. Here the vectors $\mathbf{n}$ and $\mathbf{p}$ are defined as in *Theorem 1*. Since the matrix W_J is generally not square, to find the solution for $\mathbf{s}$ we shall use the Moore-Penrose inverse. This inverse is denoted M^+ for the matrix M and has been numerically implemented by using singular value decomposition. The Moore-Penrose solution to $\mathscr{I}_J$ is $\mathbf{s} = W_J^+\mathbf{b}_J$.

The numerical inverse, W_J^+, will provide an answer even though no solutions analytically exists. To check if $W_J\mathbf{s} = \mathbf{b}_J$ has solutions we check the norm divergence of the solution, i.e. a solution exists if $|W_J W_J^+ \mathbf{b}_J - \mathbf{b}_J| < T$, where T denotes a tolerance for error. With this we construct a algorithm, assuming that $N \geq 3$. The algorithm will iterate trough partial terms $\mathscr{I}_J$, excluding all full terms containing the partial term if the partial term $|W_J W_J^+ \mathbf{b}_J - \mathbf{b}_J| \geq T$. Upon completion of the algorithm it will output a set of sets of integers $L_N = \{\{k_{11} \ldots, k_{1N}\}, \ldots, \{k_{K_N 1} \ldots, k_{K_N N}\}\}$. This set gives a numerical form of Ω, i.e. solutions to equation 3, as $\Omega = \{W_J^+\mathbf{b}_J : J \in L_N\}$.

3.3 Ambiguities to DOAs

The second step relies on fixing a DOA, $\mathbf{k}_0$, and then finding all possible vectors $\mathbf{s}_0 = \mathbf{k}_0 - \mathbf{k}$. As all solutions Ω for equation 3 are known from *Theorem 1* and the numerical calculation, all points on this surface $\mathbf{s}_0$ that coincide with Ω represent a distinct ambiguity for $\mathbf{k_0}$. This set of ambiguities is defined as

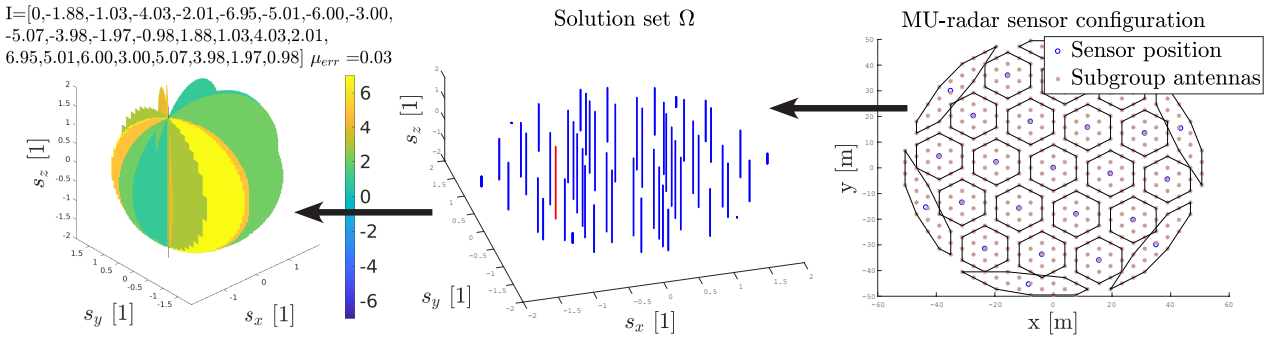

Figure 1. Right panel: MU-radar configuration. Middle panel: solution set Ω from algorithm in Section 3.2 and $T = 0.1$. Left panel: The plane intersections generating the red line highlighted in the middle panel. The title of the left panel shows $RW_J^+\mathbf{b}_J = \mathbf{I}$ and $\mu_{err} = \frac{1}{N}\sum_{i=1}^{N} |I_i - \text{round}(I_i)|$.

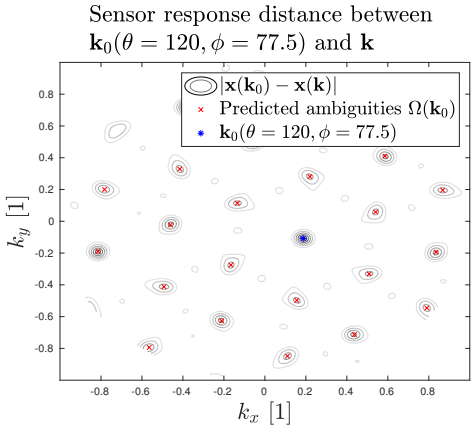

Figure 2. Red crosses indicate the set $\Omega(\mathbf{k}_0)$ of ambiguities defined in Equation 4 for $\mathbf{k}_0(\theta = 120°, \phi = 77.5°)$, which is represented by the blue star. The contours show the distance in $\mathbb{C}^N$ space between the sensor response model for $\mathbf{k}_0$ and all other $\mathbf{k}$'s, i.e $|\mathbf{x}(\mathbf{k}_0) - \mathbf{x}(\mathbf{k})|$. The contours indicate local minima in distance, ranging from 1 to 4. The rest of the DOA space in the figure has an almost constant distance of 8. All predicted ambiguities reside at local minima.

$$\Omega(\mathbf{k}_0) = \{\mathbf{s}_0 \in \Omega : \mathbf{s}_0 = \mathbf{k}_0 - \mathbf{k}\ \forall\, \mathbf{k}\}. \tag{4}$$

As a practical example we have taken the sensor configuration for the MU-radar in Japan [3] and calculated all ambiguities. Figure 1 shows an illustration of the algorithm. The right panel shows the MU-radar sensor and antenna configuration. The middle panel displays the solution set Ω obtained by running the algorithm in Section 3.2. The left panel illustrates the plane intersections generating the red line highlighted in the middle panel. The tolerance was set to $T = 0.1$ and the title of the left panel shows the integer solution for this ambiguity, defined as $RW_J^+\mathbf{b}_J = \mathbf{I}$. $\mathbf{I}$ is not a perfect integer solution, but close enough to create an *approximate* ambiguity. This effect will be discussed further in the next section.

To validate the predicted ambiguities and as an example we picked a DOA, azimuth 120° and elevation 77.5°, as $\mathbf{k}_0$ and found all intersections between the possible $\mathbf{s}_0$'s and solutions in Ω giving the set $\Omega(\mathbf{k}_0)$. Then alongside the predicted ambiguities, the distance in $\mathbb{C}^N$ between the sensor response model for $\mathbf{k}_0$ and for all other $\mathbf{k}$'s were calculated. This result is illustrated in Figure 2. The contours indicate local minima in distance, ranging from 1 to 4. The rest of the DOA space in the figure has an almost constant distance of 8. As seen in the figure, all predicted ambiguities (red crosses) reside at local minima. Thus the prediction holds, even for approximate ambiguities.

4 Model-matching algorithms

4.1 Noise-induced ambiguity

When the sensor response model has approximately the same response for several very different waves, then noise can perturb the signal from one response to another leading to misclassification of the DOA. We call this effect a noise-induced ambiguity, or approximate ambiguity. The fact that the responses are similar where a predicted ambiguity resides is illustrated in Figure 2. In this figure none of the local minima reached 0 since no intersections in Ω remained when the tolerance T was decreased towards the numerical accuracy of the computation. Thus the MU-radar has no theoretical ambiguities. Yet there are still approximate ambiguities when $T = 0.1$, which is close enough for the noise to cause misclassifications.

When analysing a signal, it is impossible to disentangle noise-induced ambiguities as we can only predict statistics of noise, not its specific values. However, if there are several measurements and the noise distribution is known, examining a distribution of DOAs can indicate what the true DOA is. Using this knowledge, the trajectory calculation can be improved. For example, one can create better outlier analysis or achieve better statistics by moving outliers that are generated by ambiguities to their correct positions. The

fitting process can also be improved when accounting for the sensor response space topology.

4.2 Sub-array gain pattern

The sub-array ideal gain pattern is defined as $\gamma_j(\mathbf{k}) = Y(\mathbf{k})\sum_{k=1}^{n_j} e^{-i\langle \mathbf{k},\rho_{jk}\rangle_{\mathbb{R}^3}}$ where Y is the individual antennas gain pattern and $\rho_{jk} = \mathbf{h}_{jk} - \mathbf{r}_j$. Modifying the sensor response model in equation 1 to account for the antenna gain pattern we get

$$\mathbf{x} = \gamma(\mathbf{k}) \odot \Psi(\mathbf{k}) = \gamma_j(\mathbf{k})\Psi(\mathbf{r}_j, t, \mathbf{k}) \tag{5}$$

where $\odot$ denotes the Hadamard product, or element-wise multiplication. This new sensor response model will not have the same ambiguities as the function in equation 1.

4.3 Using gain to resolve ambiguities

We found that for the MU-radar, the sensor response models in equation 1 and in equation 5 converge at the zenith. But they diverge substantially with decreasing elevation. Indicating that this property can be used to distinguish between a close-to-zenith detection and a far-from-zenith detection. To examine this possibility further we used the model-matching algorithm MUSIC [4]. A signal was generated using Equation 5, then two MUSIC algorithms were applied on this synthetic signal. The first MUSIC algorithm used Equation 1 as a model with output $\mathbf{k}$. The second MUSIC algorithm used Equation 5 as a model with output $\mathbf{k}'$. These two algorithms should output different results if the two sensor response models differ enough so that the closest match changes. The resulting map is displayed in Figure 3 where the colormap shows the magnitude of the plane projected distance between the two results , $\sqrt{(k_x - k'_x)^2 + (k_y - k'_y)^2}$. Below $\approx 80^\circ$ elevation, the two algorithms start producing very different results, except in certain side-lobes where the result is again identical. This result showed that if these two MUSIC algorithms are run on a detected signal and the results does not differ, the signal probably has a DOA with elevation $> 80^\circ$. This shifting effect is true regardless if noise perturbed the signal from $\mathbf{k}_0$ to a DOA from $\Omega(\mathbf{k}_0)$, as the modulation by the gain has not changed. These are the first steps toward a practical method to resolve ambiguities.

5 Conclusions

We have derived a theoretical representation of all DOA ambiguities present in any multichannel radar system. We have also developed a numerical algorithm that can calculate theoretical ambiguities and approximate ambiguities on a personal computer. We have found ambiguities that can originate from noise in otherwise ambiguity-free radar systems. The methods can be used to optimize new sensor

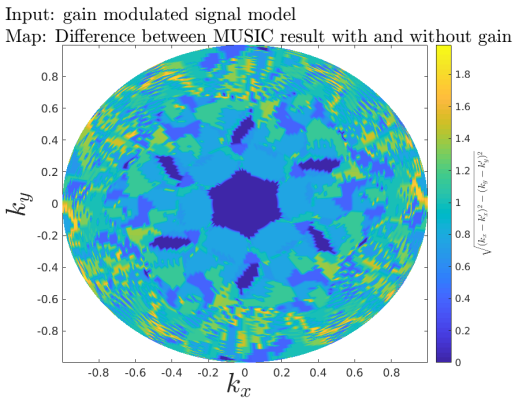

Figure 3. Synthetic signal generated using Equation 5. The first MUSIC algorithm, with output $\mathbf{k}$, used Equation 1 as a model and the second MUSIC, with output $\mathbf{k}'$, used Equation 5. The color shows the magnitude of the plane-projected distance, $\sqrt{(k_x - k'_x)^2 + (k_y - k'_y)^2}$, between the two MUSIC algorithm outputs.

configurations as it provides both an exact identification of ambiguities given a sensor configuration and a measure of how close the configuration is to forming new ambiguities. We have started development towards a method to use the additional information of sub-array gain patterns to resolve ambiguities in model-matching algorithms. This information can be used, together with statistical information, to improve trajectory estimation, identify faulty DOA calculations and correct them.

6 Acknowledgements

The MU radar belongs to and is operated by the Research Institute of Sustainable Humanosphere, Kyoto University, Japan.

References

[1] Godara, L. and Cantoni, A. (1981). Uniqueness and linear independence of steering vectors in array space. *The Journal of the Acoustical Society of America*, 70(2), pp.467-475.

[2] Kastinen, D. and Kero, J. (2017). A Monte Carlo-type simulation toolbox for Solar System small body dynamics: Application to the October Draconids. *Planetary and Space Science*, 143, pp.53-66.

[3] Kero, J., Szasz, C., Nakamura, T., Terasawa, T., Miyamoto, H. and Nishimura, K. (2012). A meteor head echo analysis algorithm for the lower VHF band. *Annales Geophysicae*, 30(4), pp.639-659.

[4] Schmidt, R. (1986). Multiple emitter location and signal parameter estimation. *IEEE Transactions on Antennas and Propagation*, 34(3), pp.276-280.